

## **Internal modifications to reduce pollutant emissions from marine engines. A numerical approach**

M.I. Lamas<sup>1</sup>, C.G. Rodríguez<sup>1</sup>, J.D. Rodríguez<sup>2</sup> and J. Telmo<sup>3</sup>

<sup>1</sup>*Department of Naval and Ocean Engineering, Universidade da Coruña, Spain*

<sup>2</sup>*Department of Industrial Engineering, Universidade da Coruña, Spain*

<sup>3</sup>*Department of Agroforestry Engineering, Universidade de Santiago de Compostela, Spain*

**ABSTRACT:** Taking into account the increasingly stringent legislation on emissions from marine engines, this work aims to analyze several internal engine modifications to reduce NO<sub>x</sub> (nitrogen oxides) and other pollutants. To this end, a numerical model was employed to simulate the operation cycle and characterize the exhaust gas composition. After a preliminary validation process was carried out using experimental data from a four-stroke, medium-speed marine engine, the numerical model was employed to study the influence of several internal modifications, such as water addition from 0 to 100% water to fuel ratios, exhaust gas recirculation from 0 to 100% EGR rates, modification of the overlap timing from 60 to 120°, modification of the intake valve closing from 510 to 570°, and modification of the cooling water temperature from 70 to 90 °C. NO<sub>x</sub> was reduced by nearly 100%. As expected, it was found that, by lowering the combustion temperature, there is a notable reduction in NO<sub>x</sub>, but an increase in CO (carbon monoxide), HC (hydrocarbons) and consumption.

**KEY WORDS:** Marine diesel engine; Emissions; Combustion; Computational fluid dynamics (CFD).

### INTRODUCTION

Over the last few years, as concern about air pollution increases, several legislative measures have been taken. In terms of marine engines, the Environmental Protection Agency and the European Commission limit emissions in the United States and the European Union respectively. On an international level, the International Maritime Organization (IMO) has set up and maintained a comprehensive regulatory framework for shipping. In 1973, the IMO adopted Marpol 73/78, the International Convention for the Prevention of Pollution from Ships, designed to reduce marine pollution. Particularly, Marpol Annex VI places limits on SO<sub>x</sub> (sulphur oxides) and NO<sub>x</sub>. With the former, it limits the sulphur content of fuels. For the latter, it establishes a curve that indicates maximum allowable NO<sub>x</sub> emission levels depending on engine speed, geographical area and manufacturing data.

Due to the special attention that legislation pays to NO<sub>x</sub> emitted from marine engines, various reduction methods have been developed over recent years. The main factors influencing NO<sub>x</sub> formation are concentrations of oxygen and nitrogen, along with local temperatures in the combustion process. Therefore, internal engine modifications focus on lowering oxygen and nitrogen concentrations, peak temperature and the amount of time in which combustion gases remain at high temperatures.

---

Corresponding author: M.I. Lamas, e-mail: [isabellamas@udc.es](mailto:isabellamas@udc.es)

This is an Open-Access article distributed under the terms of the Creative Commons Attribution Non-Commercial License (<http://creativecommons.org/licenses/by-nc/3.0>) which permits unrestricted non-commercial use, distribution, and reproduction in any medium, provided the original work is properly cited.

A very common internal modification to reduce  $\text{NO}_x$  from marine engines is water addition. This measure reduces  $\text{NO}_x$  formation for two reasons. The specific heat capacity of the cylinder gases is increased because water has higher specific heat capacity than air. Moreover, the overall oxygen concentration is reduced. Water's effects will vary with the engine type, but generally 1% percent of water reduces  $\text{NO}_x$  by 1%, Woodyard (2009).

Another common way to reduce  $\text{NO}_x$  emissions is exhaust gas recirculation (EGR). This lowers the combustion temperature, and, consequently,  $\text{NO}_x$ , by recirculating a portion of the exhaust gases to the charge air. As is the case with water addition, EGR reduces  $\text{NO}_x$  formation due to an increase in the specific heat capacity of the cylinder gases and reduced overall oxygen concentration. Geist et al. (1998) found a 22%  $\text{NO}_x$  reduction with 6% EGR in the Wärtsilä 4RTX54 research engine. However, they postulated that EGR increases smoke, HC and CO. Millo et al. (2011) analyzed EGR combined with other modifications in a Wärtsilä W20 marine engine and obtained  $\text{NO}_x$  reductions of up to 90%.

Another way to reduce  $\text{NO}_x$  is by modifying the injection pattern. In this way, a delayed injection leads to lower peak pressures and, therefore, temperatures. Retarding injection timing also decreases the amount of fuel burnt before the peak pressure, thus reducing the residence time. Okada et al. (2001) applied an injection timing retard of  $7^\circ$  to the MAN B&W 4T50MX research engine and obtained a  $\text{NO}_x$  reduction of about 30% and an increment in consumption of about 7%. Li et al. (2010) also analyzed the influence of the fuel injection advance angle on  $\text{NO}_x$  emissions. In another study, Moreno Gutiérrez et al. (2006) looked at consumption and  $\text{NO}_x$  emissions in several marine engines with different injection timings. Al-Sened and Karini (2001) found that pre-injection can be used to shorten the delay period and thus decrease the temperature and pressure during the early stages of combustion, resulting in reduced  $\text{NO}_x$ . Fankhauser and Heim (2001) also found that pre-injection reduces  $\text{NO}_x$  with a slight increase in fuel consumption. They studied a Sulzer RT-Flex common rail engine. With triple injection, they injected the fuel charge in separate, short sprays in succession. With sequential injection, each of the three nozzles in a cylinder was actuated with different timing. The results showed about a 30%  $\text{NO}_x$  reduction with about an 8% increase in fuel consumption.

In addition to these engine modifications, downstream cleaning techniques are also commonly employed to remove  $\text{NO}_x$  and other pollutants from exhaust gases. According to Sulzer (1994), MAN B&W (1997), Caterpillar (2001) and Wärtsilä (2002), SCR can eliminate more than 90% of the  $\text{NO}_x$ . The drawbacks of using catalytic converters in ships are well known. Reducing agents are required and the catalytic reactor takes up additional space, making catalytic converters unsuitable for marine diesel engines. Consequently, modifying the internal engine is the best option for reducing the formation of pollutants on board ships.

The aim of the present work was to analyze the potential of internal engine modifications to reduce  $\text{NO}_x$  and other pollutants in the Wärtsilä 6 L 46 marine engine. For the purpose, a Computational Fluid Dynamics (CFD) software was employed. Due to its importance, special attention was given to  $\text{NO}_x$ . Consumption and emissions of HC and CO were analyzed too. A validation process was carried out with experimental measurements performed on a Wärtsilä 6 L 46 engine installed on a tuna fishing vessel. The numerical model was employed to assess the effects of different internal modifications such as water addition, exhaust gas recirculation and modification of the overlap timing, intake valves closing and cooling water temperature. As its main contribution, this paper shows the effect of several modifications using the same engine. It thus provides an objective criterion to evaluate each  $\text{NO}_x$  reduction measurement. Furthermore, this model is a cheap and fast tool for simulating a huge amount of possible configurations. In contrast, experimental tests with marine engines are expensive and laborious.

## DESCRIPTION OF THE ENGINE AND NUMERICAL PROCEDURE

The Wärtsilä 6 L 46 studied in the present work is a four-stroke, medium-speed marine diesel engine with six cylinders. Each cylinder has two intake and two exhaust valves. The operating cycle is shown in Fig. 1. After combustion has taken place, the piston descends on the power stroke with all the valves closed, Fig. 1(a). The exhaust valves open at almost the end of the power stroke and combustion gases begin to be expelled. After reaching bottom dead center (BDC), the piston rises, the intake valves open as well and fresh air enters the cylinder while combustion gases continue being expelled, Fig. 1(b). After reaching top dead center (TDC), the piston descends again and the exhaust valves are closed, Fig. 1(c). Finally, during the compression stroke, Fig. 1(d), the intake valves are closed. At the end of the compression stroke, combustion takes place and the cycle starts again.

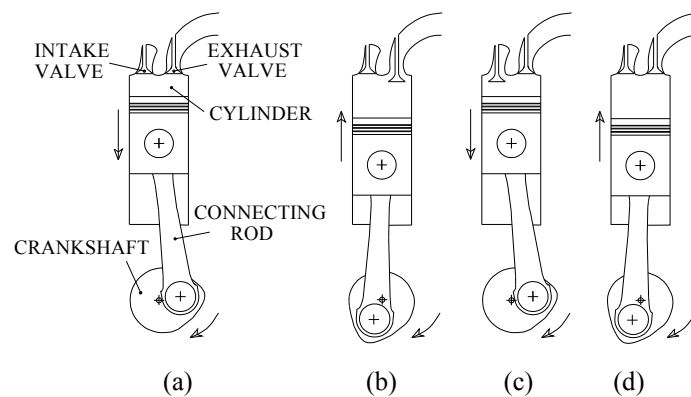


Fig. 1 Engine operation: (a) power stroke, (b) exhaust stroke, (c) intake stroke and (d) compression stroke.

The numerical simulation was developed in Lamas et al. (2012), with the exception of the combustion process, which was treated in Lamas and Rodríguez (2013). Both works employed the commercial software ANSYS Fluent for the numerical computations and SolidEdge for the CAD 3D design. Fig. 2 shows the computational mesh at the crankshaft angle position corresponding to BDC.

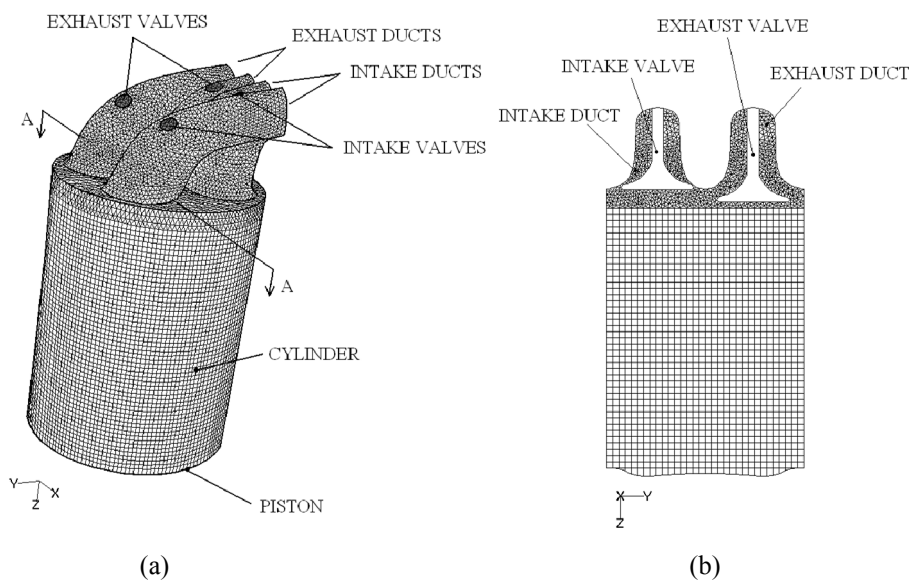


Fig. 2 Computational mesh at BDC. (a) 3D view; (b) AA section.

The Lamas et al. (2012) and Lamas and Rodríguez (2013) models can be joined to simulate the entire operating cycle. These results and a comparison with experimental data are shown in Fig. 3. This figure represents the experimentally and numerically obtained results for in-cylinder pressure, in logarithmic scale, against the piston position. In this figure, the experimental results were obtained using the MALIN 6000 (Malin Instruments, Ltd.) engine performance analyzer. As can be seen, a good concordance was obtained. Assuming the reference was in the TDC at the beginning of the power stroke, the exhaust valves open at  $127^\circ$  and close at  $404^\circ$ , while the intake valves open at  $310^\circ$  and close at  $566^\circ$ . There is a valve overlap period, between  $310^\circ$  and  $404^\circ$ , in which all the valves are opened at the same time.

Another comparison between the numerical and experimental results is given in Figs. 4(a) and (b). These figures show a satisfactory correspondence between both procedures. According to the NO<sub>x</sub> Technical Code, the tests correspond to the E2 cycle, that is, a constant engine speed is kept. Fig. 4(a) provides the SFOC (Specific Fuel Oil Consumption) and NO<sub>x</sub>, HC and CO emissions against the start of injection. Numerically, the SFOC was computed as the relation between consumption and the indicated power. The indicated power was obtained from the indicated work, which is the area under the pressure-volume diagram. A conclusion obtained from Fig. 4(a) is that delayed injection timing reduces NO<sub>x</sub> but increases SFOC, CO and HC.

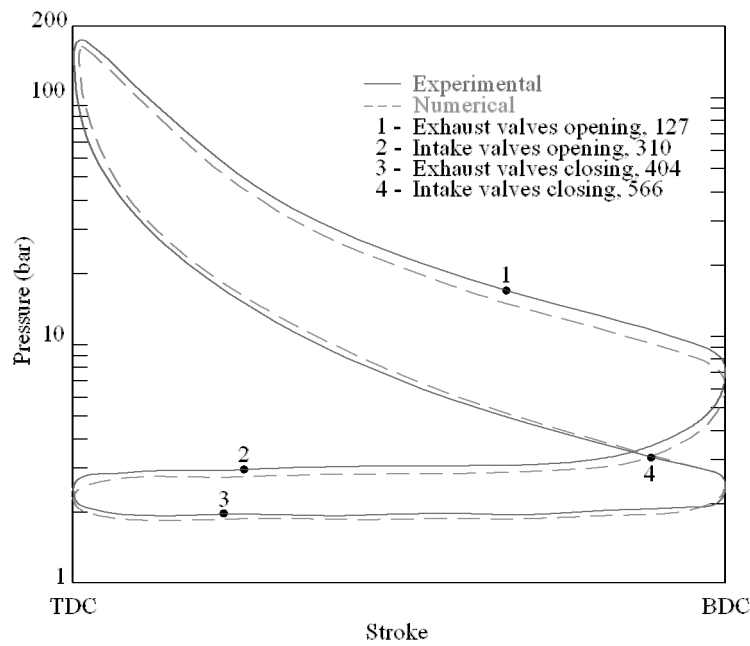


Fig. 3 In-cylinder pressure numerically and experimentally obtained at 96% load.

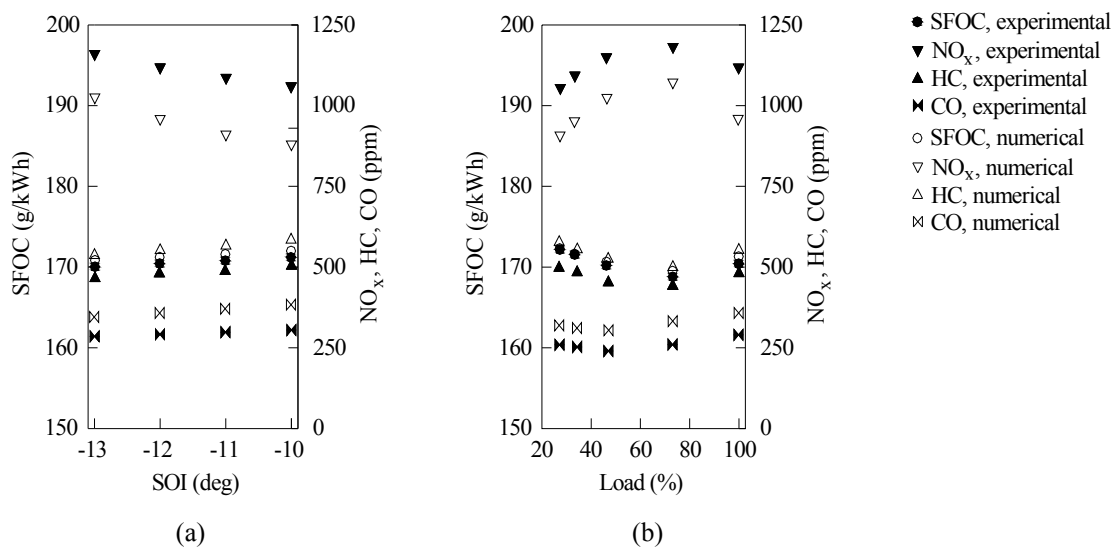


Fig. 4  $NO_x$ , CO and HC emissions experimentally and numerically obtained, (a) against the start of injection; (b) against the load.

Briefly, a delayed injection leads to less burning time and, consequently, less  $NO_x$  is produced. It also reduces temperature and pressure and, consequently, there is greater SFOC. Retarding injection timing increases HC and CO emissions because a shorter burning time causes deficient combustion.

Fig. 4(b) shows the SFOC and emissions of  $NO_x$ , HC and CO against the load. Experimentally, the  $NO_x$ , HC and CO emissions were measured using the G4100 (Green Instruments), Gasboard-3040 (Wuhan Cubic) and Gasboard-3050 (Wuhan Cubic) analyzers, respectively. This figure also shows a good concordance between experimental and numerical results. It can be seen that  $NO_x$  increases with load and then decreases. At approximately an 80% load, the temperature is at its maximum and, consequently,  $NO_x$  emissions are as well. At a low load, there is not enough fuel to promote high temperatures. However, at a high load, a rich combustion takes place, producing temperatures lower than the maximum reachable ones. SFOC also increases and then decreases with load because the power is at its maximum at high temperatures and pressures. As for CO and HC, they increase with load due to the incomplete combustion which occurs with rich mixtures.

RESULTS AND DISCUSSION

Once it was validated, the numerical model was employed to study several internal modifications such as water addition, exhaust gas recirculation and modification of the overlap timing, intake valves closing and cooling water temperature. Results are shown below.

Water addition

In practical applications, there are three possible ways to introduce water into the combustion chamber, introducing it into the charge air as humidity, through direct injection in the cylinder or through a water-fuel emulsion. In this work, water addition was simulated as an injection of a water-fuel emulsion. A water to fuel ratio, Eq. (1), between 0 to 100%, was analyzed. The results of NO<sub>x</sub>, HC, CO and SFOC against the air to fuel ratio are shown in Fig. 5. In order to be of greater relevance, the emissions are indicated in g/kWh instead ppm.

$$\text{Water to fuel ratio (\%)} = \frac{\text{mass of water}}{\text{mass of fuel}} 100 \tag{1}$$

As can be seen in Fig. 5, water addition reduces NO<sub>x</sub> but increases CO, HC and SFOC. Water absorbs energy for evaporation, increases the specific heat capacity of the cylinder gases (H<sub>2</sub>O and CO<sub>2</sub> have higher specific heat capacity than air), and reduces the overall oxygen concentration. This in turn leads to an increase in the number of moles in the gases that must be raised to combustion temperatures to make a given amount of oxygen react with fuel. Water also reduces the availability of oxygen for the NO<sub>x</sub> forming reactions. The increase in HC and CO is caused by the lower temperatures, which trigger slow combustion and partial burning. SFOC is also increased due to the lower peak pressure, which promotes lower power. The in-cylinder temperatures at a -5° crankshaft angle (5° before TDC) without water addition and with 50% water addition are indicated in Fig. 6. As can be seen, water addition notably reduces the combustion temperature.

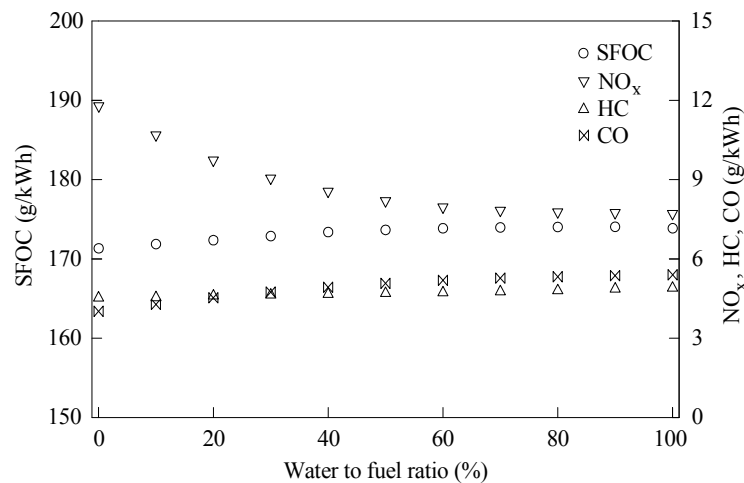


Fig. 5 SFOC, NO<sub>x</sub>, HC and CO against the water to fuel ratio.

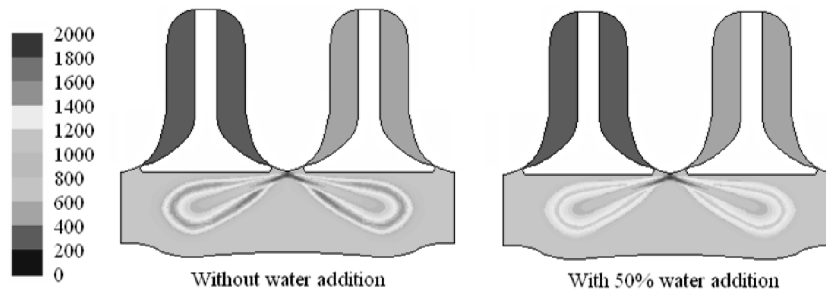


Fig. 6 Temperature field (°C) at -5° crankshaft angle, without water addition and with 50% water addition.

### Exhaust Gas Recirculation (EGR)

EGR involves mixing a portion of the exhaust gas into the intake air to constitute a mixture of air and inert gases with a lower local oxygen concentration. The results of NO<sub>x</sub>, HC, CO and SFOC against the EGR rate, Eq. (2), are shown in Fig. 7.

$$\text{EGR rate (\%)} = \frac{\text{mass of recirculated exhaust gas}}{\text{mass of total intake mixture}} 100 \quad (2)$$

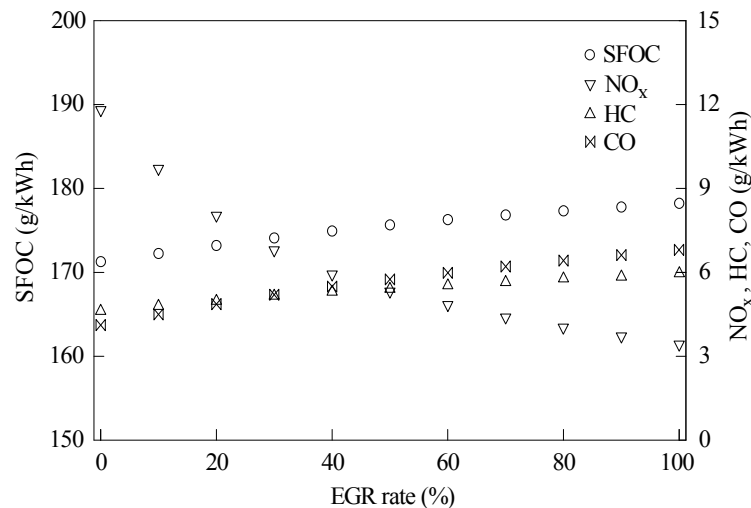


Fig. 7 SFOC, NO<sub>x</sub>, HC and CO against the EGR rate.

As can be seen in Fig. 7, EGR lowers NO<sub>x</sub> emissions but increases HC, CO and SFOC. Recirculated exhaust gasses displace the fresh air entering the combustion chamber. As a result of this air displacement, a lower amount of oxygen in the intake mixture is available for combustion. In other words, the air-fuel ratio is lowered. In addition, mixing exhaust gases with the intake air increases the specific heat of the intake mixture. This results in a lower flame temperature. For this reasons, NO<sub>x</sub> is highly reduced. As indicated, EGR is an effective method for NO<sub>x</sub> control. Nevertheless, practical applications do not usually use more than 50% of the EGR rate because particles from the exhaust gasses damage the engine, Lamas and Rodríguez (2012).

The increase in HC and CO with EGR is caused by lower temperatures and the reduced amount of oxygen available for reactions, which promote slow combustion and partial burning. SFOC is increased with EGR due to the lower peak pressure which supposes lower power.

Another NO<sub>x</sub> reduction method related to intake air involves using a correction factor, known as  $k_{\text{HIDIES}}$ , for humidity and temperature. This remains out of the scope of the present work.

### Modification of the overlap timing

The CFD model was also employed to analyze different values for the overlap timing. The overlap timing is the interval of time in which the intake and exhaust valves are both open. The results are shown in Fig. 8. In this figure, the intake valves' opening angle and the exhaust valves' closing angle were increased and reduced by the same amount.

As can be seen in Fig. 8, NO<sub>x</sub> emissions increase with the overlap timing, while CO, HC and SFOC decrease. The overlap period mainly affects the scavenging of the combustion gases, Puskar and Bigos (2010). With short overlap timings, a high quantity of residual gas is retained in the cylinder. For this reason, NO<sub>x</sub> emissions are low during short overlap timings and increase as the overlap timing is raised. HC and CO decrease with the overlap duration. During short overlap timings, combustion is poor and incomplete due to the high quantity of residual gas. However, combustion improves as the overlap timing is extended. SFOC decreases with the overlap timing due to lower temperatures and pressures reached during longer overlap timings.

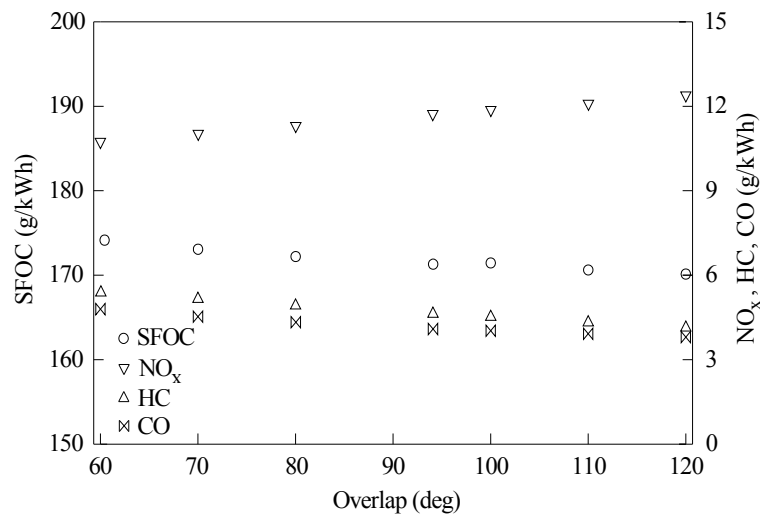


Fig. 8 SFOC, NO<sub>x</sub>, HC and CO against the overlap timing.

**Modification of the intake valves closing**

Another way to reduce NO<sub>x</sub> emissions is by advancing the intake valves closing. The results are shown in Fig. 9.

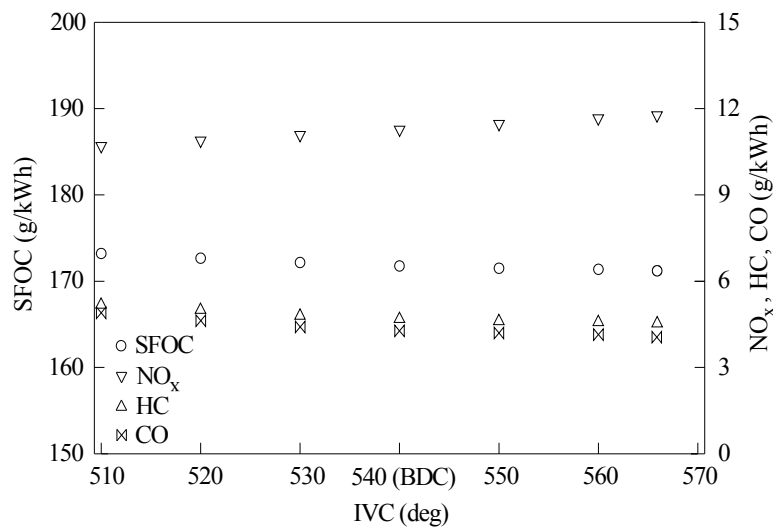


Fig. 9 SFOC, NO<sub>x</sub>, HC and CO against the instant in which intake valves close.

As can be seen in Fig. 9, NO<sub>x</sub> emissions increase as the intake valves closing is delayed. When the intake valves are closed earlier, more air is trapped in the cylinder. Consequently there are higher combustion temperatures associated with higher NO<sub>x</sub> emissions. Nevertheless, with a later intake valves closing, there is a lower quantity of air inside the cylinder. The consequence is a lower temperature and lower NO<sub>x</sub> emissions. Concerning HC and CO, they decrease as the intake valve closing is delayed due to the incomplete combustion associated with a higher quantity of exhaust gasses. In the case of BSFC, it decreases as intake valve closing is delayed due to higher pressures.

**Modification of the cooling water temperature**

The last measure proposed to reduce NO<sub>x</sub> emissions entails reducing the cooling water temperature. In the numerical model, the cooling water temperature appears as a boundary condition at the cylinder wall. The heat transferred from the cylinder to the cooling water is given by the following expression:

$$q = h(T_{gas} - T_{water}) \quad (3)$$

where  $q$  is the heat transferred,  $T_{gas}$  the in-cylinder temperature,  $T_{water}$  the cooling water temperature (78 °C) and  $h$  the heat transfer coefficient. The last is given by the following expression, Taylor (1985), which considers the effects of both convection and radiation:

$$h = 10.4kb^{-1/4}(u_{piston}/\nu)^{3/4} \quad (4)$$

where  $b$  is the cylinder bore,  $k$  the thermal conductivity of the gas,  $u_{piston}$  the mean piston speed and  $\nu$  the kinematic viscosity of the gas. Substituting values into the equation above yields  $h = 4151 \text{ W/m}^2\text{K}$ .

The results for different values for the cooling water temperature are shown in Fig. 10. As expected,  $\text{NO}_x$  emissions increase as the cooling water is increased. Nevertheless, CO, HC and SFOC decrease with the cooling water temperature due to poor combustion.

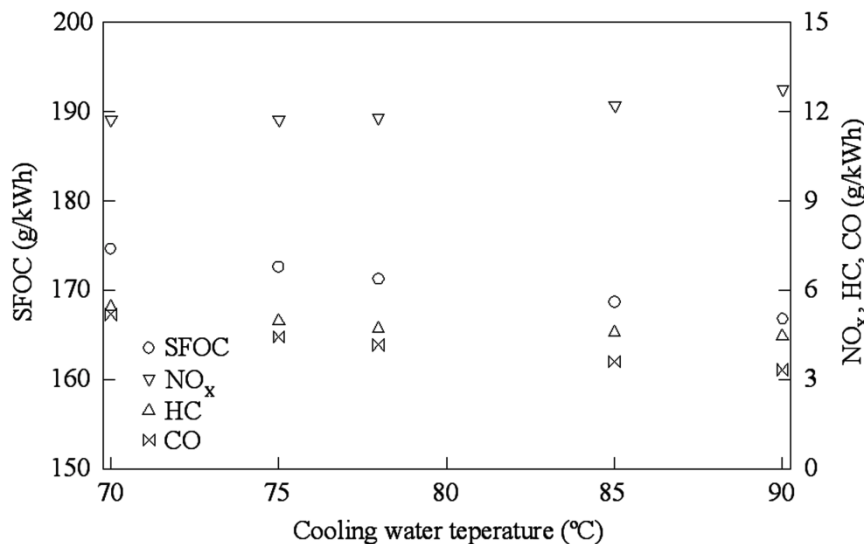


Fig. 10 SFOC,  $\text{NO}_x$ , HC and CO against the cooling water temperature.

## CONCLUSIONS

In the present paper, a numerical model was employed to analyze the potential emission reduction capabilities of several internal engine modifications. The driving force of this study was legislation related to  $\text{NO}_x$  emissions from marine engines. Also analyzed were consumption and CO and HC emissions. The  $\text{NO}_x$ -reducing modifications studied here involved water addition, exhaust gas recirculation, modification of the overlap timing, modification of the intake valve closing and modification of the cooling water temperature. As its main contribution, this paper provides a cheap and fast tool for studying the effect of several  $\text{NO}_x$  reduction measurements. On the other hand, experimental tests are too expensive and laborious for marine engines. A four-stroke marine engine, the Wärtsilä 6 L 46, was chosen for the computations. Experimental measurements from this model installed on a tuna fishing vessel were employed to validate the numerical model.

The numerical model showed that a reduction in the combustion temperature notably reduces  $\text{NO}_x$  but increases CO, HC and consumption. A  $\text{NO}_x$  reduction of almost 100% with a fuel penalty of 4.6% was obtained using EGR. Water addition also lead to a significant  $\text{NO}_x$  reduction with a fuel penalty of 1.7%. Nevertheless, in practical applications, the EGR rate poses limitations, as does the water to fuel ratio in terms of engine performance. The remaining modifications- related to modification of the overlap timing, intake valve closing and cooling water temperature- provided lower  $\text{NO}_x$  reductions.



## ACKNOWLEDGEMENTS

The authors would like to express their gratitude to “Talleres Pineiro, S.L.”, marine engines maintenance and repair shop.

## REFERENCES

- Al-Sened, A. and Karimi, E., 2001. Strategies for NO<sub>x</sub> reduction in heavy duty engines. *Proceedings of the 23<sup>rd</sup> CIMAC Congress*, Hamburg, Germany, 7-10 May 2001.
- Caterpillar, 2001, The green ship: inside emission technology. *Marine Engineers Review*, November 2001, pp.46-47.
- Fankhauser, S. and Heim, K., 2001. The Sulzer RT-flex launching the era of common rail on low speed engines. *Proceedings of the 23<sup>rd</sup> CIMAC Congress*, Hamburg, Germany, 7-10 May 2001.
- Fluent 6.3, 2006. *Documentation*. NH: Fluent Inc.
- Geist, M., Holtbecker, R. and Chung, S.Y., 1997. Marine diesel NO<sub>x</sub> reduction technique - A new Sulzer diesel Ltd approach. *Proceedings of the 1997 International Congress and Exposition*, Detroit, United States, 24-27 February 1997.
- Lamas, M.I. and Rodríguez, C.G., 2013. Numerical model to study the combustion process and emissions in the Wärtsilä 6L 46 four-stroke marine engine. *Polish Maritime Research*, 20(2), pp.61-66.
- Lamas, M.I., Rodríguez, C.G. and Rebolledo, J.M., 2012. Numerical model to study the valve overlap period in the Wärtsilä 6L 46 four-stroke marine engine. *Polish Maritime Research*, 19(1), pp.31-37.
- Lamas, M.I. and Rodríguez, C.G., 2012. Emissions from marine engines and NO<sub>x</sub> reduction methods. *Journal of Maritime Research*, 9(1), pp.77-82.
- Li, K., Li, B. and Sun, P., 2010. Influence of fuel injection advance angle on nitrogen oxide emission from marine diesel engine. *Journal of Dalian Maritime University*, 36(3), pp.87-89.
- MAN B&W, 1997. Emission Control of two-stroke low-speed diesel engines, *MAN B&W Technical Paper*.
- Millo, F., Bernardi, M.G. and Delneri, D., 2011. Computational analysis of internal and external EGR strategies combined with Miller cycle concept for a two stage turbocharged medium speed marine diesel engine, *SAE Paper 2011-01-1142*.
- Moreno Gutiérrez, J., Rodríguez Maestre, I., Shafik, T., Durán Grados, C.V. and Cubillas, P.R., 2006. The influence of injection timing over nitrogen oxides formation in marine diesel engines. *Journal of Marine Environmental Engineering*, 8(4), pp.299-308.
- Okada, S., Hamaoka, S., Akimoto, S., Masakawa, S., Takeshita, K., Seki, M., Yoshikawa, S. and Yonezawa, T., 2001. The development of very low fuel consumption medium speed diesel engine. *Proceedings of the 23<sup>rd</sup> CIMAC Congress*, Hamburg, Germany, 7-10 May 2001.
- Puskar, M. and Bigos, P., 2010. Output performance increase of two-stroke combustion engine with detonation combustion optimization. *Strojarstvo*, 52 (5), pp.577-587.
- Sulzer, 1994, Exploring the effects of SCR on a two-stroke engine. *Marine Engineers Review*, Issue June 1994, pp.12-14.
- Taylor, C.F., 1985. *The internal combustion engine in theory and practice*. 2nd ed. Massachusetts: MIT Press.
- Wärtsilä NSD, 2001. *Wärtsilä 46. Project guide for marine applications*. Wärtsilä NSD
- Wärtsilä NSD, 2002. *Sulzer RT-flex60C Technology Review*. Wärtsilä NSD
- Woodyard, D., 2009. *Pounder's marine diesel engines and gas turbines*. 9rd ed. Oxford: Elsevier.